Optimum Aeroelastic Design of Flapping Wing for Micro Air Vehicles

Koji Isogai, Yuichi Kamisawa, Yohei Harino, and Hiroyuki Sato
Nippon Bunri University
1727 Oaza Ichigi, Oita, Japan

Abstract

A method is presented for the optimum aeroelastic design of a flapping wing employing lifting-surface theory as an aerodynamic tool and the complex method as the optimization algorithm. The method is applied to the optimum design of a flapping wing of a Kite Hawk (Milvus migrans) UAV and the optimum thickness distribution of the main-spar is determined. As the result of the optimization, a high propulsive efficiency of 75% is attained considering only dihedral flapping of the main spar. By evaluating the viscous effect for this optimum design using a three-dimensional Navier–Stokes code, the effectiveness of the design is confirmed.

I. Introduction

Bird-type aerial vehicles with flapping wings have attracted considerable interest for their possible use in wide ranging monitoring and surveillance activities. Although several such vehicles have been developed to date, most have employed membrane type wings. However, membrane wings are not efficient since the feathering (twisting) motion, which is essential for efficient flapping flight, does not occur in an ideal manner (a 90 deg advance phase angle of feathering motion ahead of flapping motion is usually the most efficient). However, Delaurier and Harris [1, 2] have developed an ornithopter that has double solid surface airfoil sections and uses aeroelastic deformation to generate a twisting motion by dihedral flapping. To obtain favorable aeroelastic deformation, they developed a design program called ComboWing that determines the optimum aeroelastic design of a flapping wing. They employed strip theory as an aerodynamic tool and conducted the optimization manually, without using an automated optimization algorithm.

The purpose of the present study is to develop an automated optimum aeroelastic design method using a more accurate aerodynamic tool, namely, unsteady lifting-surface theory. The new method is then applied to the design of the flapping wing of a Kite Hawk (Milvus migrans) UAV (Unmanned Air Vehicle). The optimum design thus obtained is examined by numerical simulation using a

three-dimensional Navier–Stokes code.

II. Equations of Motion for Elastic Flapping Wing and Solution Procedure Using Doublet Lattice Method

In this section, the basic equations of motion for an elastic flapping wing are derived using Lagrange's equations of motion. The solution procedure using the Doublet Lattice Method (DLM) [3] as the aerodynamic tool is also described. In Fig. 1, the coordinates and the definition of the wing displacement are shown. In the figure, T is time and F(X,Y,T) is the displacement of the wing mean surface at an arbitrary point (X,Y) on the wing. F can be expressed by the following equation:

$$F(X,Y,T) = F_r(X,Y,T) + \sum_{i=1}^{N} \phi_i(X,Y) q_i(T) \qquad (1)$$

where $F_r(X,Y,T)$ is the displacement of the rigid wing due to forced oscillation, $\phi_i(X,Y)$ is the i-th natural vibration mode of the wing and $q_i(T)$ is the i-th generalized coordinate of the elastic deformation. For this wing displacement, the kinetic energy of the wing can be expressed as

$$K = \iint_S \tfrac{1}{2} m(X,Y)(dZ/dT)^2 \, dXdY \qquad (2)$$

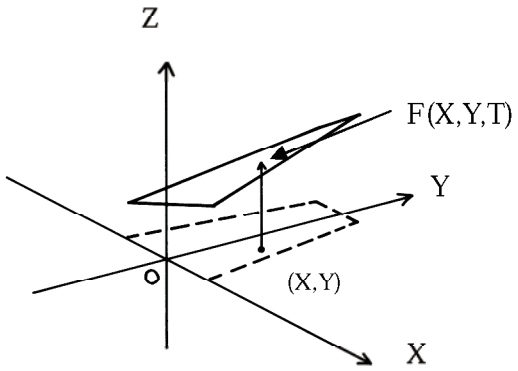

Fig. 1 Definitions of coordinates.

where m(X,Y) is the wing mass per unit area and where $\iint_S$ represents the surface integral on the full span wing area. The strain energy of the wing can be expressed as

$$U = \tfrac{1}{2} \omega_i^2 M_i q_i^2(T) \qquad (3)$$

where ω_i is the i-th natural circular frequency of the wing, and where M_i is the generalized mass given by

$$M_i = \iint_S m(X,Y)\phi_i^{\,2}(X,Y)dXdY \qquad (4)$$

The virtual work done by the external force (aerodynamic force) due to the virtual displacement δq_i of the i-th generalized coordinate can be given by

$$\delta W = \iint_S \Delta P(X,Y,T)\phi_i(X,Y)dXdY\delta q_i \qquad (5)$$

where ΔP is the pressure difference between the upper and lower surfaces of the wing. From Eq. (5) and by the definition of the generalized force Q_i, that is $\delta W=Q_i\delta q_i$, Q_i can be given by

$$Q_i = \iint_S \Delta P(X,Y,T)\phi_i(X,Y)dXdY \qquad (6)$$

Substituting Eqs. (2), (3) and (6) into Lagrange's equations of motion, we finally obtain the general expressions for the equation of motion of an elastic flapping wing as

$$M_i(d^2q_i/dT^2) + \omega_i^{\,2}M_iq_i =$$

$$-\iint_S m(X,Y)\phi_i(X,Y)(d^2F_r(X,Y,T)/dT^2)dXdY$$

$$+\iint_S \Delta P(X,Y,T)\phi_i(X,Y)dXdY, \quad i=1,\ldots,N \qquad (7)$$

In deriving Eq. (7), we use the orthogonal condition of the natural vibration modes. In Eq. (7), the displacement $F_r(X,Y,T)$ of the rigid wing or the forced oscillation of the un-deformed wing can be expressed as

$$F_r(X,Y,T) = (H_r + \phi_0 Y)\cos(\omega T) - (\theta_r + b_\theta Y)(X-A)\cos(\omega T + \phi) \qquad (8)$$

where H_r and θ_r are the amplitudes of the heaving and pitching oscillations at the root station, respectively, ϕ_0 is the flapping oscillation amplitude, b_θ is the rate of twist of the feathering oscillation amplitude, A is the X coordinate of the feathering axis and ϕ is the advance phase angle of the feathering oscillation ahead of the flapping oscillation. (See also Fig. 2 for the definitions of flapping wing motion.)

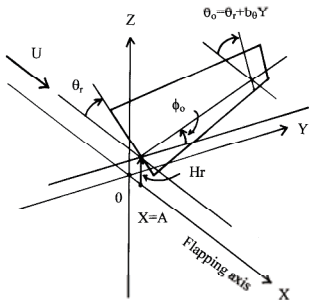

Fig. 2 Definitions of wing motion.

The load distribution $\Delta P(X,Y,T)$ is expressed as

$$\Delta P(X,Y,T) = \tfrac{1}{2}\rho U^2\{\Delta C_P^{(F)}(X,Y,T) + \sum_{j=1}^{N}\overline{\Delta C_{Pj}}(X,Y)q_j(T)\} \qquad (9)$$

where $\Delta C_P^{(F)}$ is the pressure difference coefficient due to the rigid wing displacement and $\overline{\Delta C_{Pj}}$ is the pressure difference coefficient due to the j-th natural vibration mode. By assuming sinusoidal wing motion and introducing a complex expression, $\Delta C_P^{(F)}$ and q_j can be expressed as

$$\Delta C_P^{(F)}(X,Y,T) = \overline{\Delta C_P^{(F)}}(X,Y)e^{i\omega T} = \overline{\Delta C_P^{(F)}}e^{ikt}$$

$$q_i = \overline{q_i}e^{i\omega T} = \overline{q_i}e^{ikt} \qquad (10)$$

where $\overline{\Delta C_P^{(F)}}$ and $\overline{q_i}$ are complex quantities.

$F_r(X,Y,T)$ of Eq. (8) can be expressed as

$$F_r(X,Y,T) = (H_r + \phi_0 Y)e^{i\omega T} - (\theta_r + b_\theta Y)(X-A)e^{i(\omega T+\phi)} \qquad (11)$$

By substituting Eqs. (9), (10) and (11) into Eq. (7), and by non-dimensionalizing Eq. (7) using the root semichord b_0, we obtain the matrix form of Eq. (7) as

$$\left\{\left[(\omega_i/\omega)^2 - 1\right] - \left[A_{ij}\right]\right\}\left\{\overline{q_j}\right\} = \left\{\overline{F_i}\right\} \qquad (12)$$

where

$$A_{ij} = \frac{1}{k^2}\left(\frac{\rho b_0^4}{M_i}\right)\left\{\int_0^s\int_{\xi_l}^{\xi_t}\overline{\Delta C_{pj}}(x, y)\phi_i(x, y)dxdy\right\} \qquad (13)$$

$$\overline{F_i} = \frac{2b_0^3}{M_i}\int_0^s\int_{\xi_l}^{\xi_t} m(x, y)(h_r + \phi_0 y - (\theta_r + b_\theta z)(x - a)e^{i\phi})\phi_i(x, y)dxdy$$

$$+\frac{1}{k^2}\left(\frac{\rho b_0^4}{M_i}\right)\int_0^s\int_{\xi_l}^{\xi_t}\overline{\Delta C_p^{(F)}}(x, y)\phi_i(x, y)dxdy \qquad (14)$$

$\overline{\Delta C_{pj}}$ can be computed by solving the integral equations of the lifting-surface theory [3], namely,

$$(ik\phi_j + \frac{\partial\phi_j}{\partial x})/b_0 = \frac{1}{8\pi}\iint_S \overline{\Delta C_{pj}}(\xi,\eta)K_{WT}(x, y;\xi,\eta)d\xi d\eta \qquad (15)$$

where K_{WT} is the kernel function. Similarly, $\overline{\Delta C_p^{(F)}}$ in Eq. (14) can be found by solving the integral equation of the lifting surface theory [3], namely,

$$ik(h_r + \phi_0 y - (\theta_r + b_\theta y)(x - a)e^{i\phi}) - (\theta_r + b_\theta y)e^{i\phi} = \frac{1}{8\pi}\iint_S \overline{\Delta C_p^{(F)}}(\xi,\eta)K_{WT}(x, y;\xi,\eta)d\xi d\eta \qquad (16)$$

In Eqs. (13)–(16), x, y, ξ and η are dimensionless coordinates obtained by dividing the physical coordinates by b_0, a is the x coordinate of the feathering axis, h_r is the dimensionless heaving amplitude at the root station, ξ_l and ξ_t are the x coordinates of the leading and trailing edges, respectively, and s is defined by l/b_0 with l the semi-span length. We employ the DLM to solve Eqs. (15) and (16).

By solving Eq. (12) for a given forced motion and the natural vibration characteristics of the wing, we can compute the load distributions $\Delta P(X, Y, T)$ using Eq. (9) in complex form as

$$\overline{\Delta P}(x, y)e^{ikt} = \tfrac{1}{2}\rho U^2\overline{\Delta C_p}(x, y)e^{ikt} = \tfrac{1}{2}\rho U^2(\overline{C_p^{(F)}}(x, y) + \sum_{j=1}^{N}\overline{\Delta C_{pj}}(x, y)\overline{q_j})e^{ikt} \qquad (17)$$

Once $\Delta P(x, y, t)$ is given, the time averaged thrust and necessary power can be computed as follows. The time averaged thrust $\overline{T}$ is composed of two components, the leading edge suction $\overline{T_L}$ and the thrust induced by tilting the normal force vector due to the feathering motion $\overline{T_D}$:

$$\overline{T} = \overline{T_L} + \overline{T_D} \tag{18}$$

$$\overline{T} = \tfrac{1}{2}\rho U^2 S\overline{C_T} = \tfrac{1}{2}\rho U^2 S(\overline{C_{TL}} + \overline{C_{TD}}) \tag{19}$$

where $\overline{C_{TL}}$ is the thrust coefficient due to leading edge suction and $\overline{C_{TD}}$ is the thrust coefficient due to the tilt of the normal force vector. $\overline{C_{TL}}$ can be computed by a procedure similar to that proposed by Lan [4] for the quasi-vortex lattice method.

First, we compute the leading-edge singularity parameter [4] $\overline{C_S}$ using $\overline{\Delta C_p}$ in Eq. (17):

$$\overline{C_S}(y) = \tfrac{1}{2}\overline{\Delta C_p}(x_{l,lp}, y)\sqrt{\frac{(x_{l,lp} - x_l)}{2}} \tag{20}$$

where $x_{l,lp}$ is the x coordinate of the midpoint of the lifting line of the leading edge panel [3] and x_l is the x coordinate of the leading edge. It should be noted that $x_{l,lp}$ and x_l are functions of y. Using $\overline{C_S}$ thus determined, we finally compute $\overline{C_{TL}}$ as

$$\overline{C_{TL}} = \frac{2b_0^2}{S}\int_0^s \left\{\pi\overline{C_s^2}/(2\cos\Lambda_e)\right\}C(y)dy \tag{21}$$

where C(y) is the dimensionless local chord length and Λ_e is the sweep angle of the quarter chord line of the leading edge panel. In Eq. (21), $\overline{C_S^2}$ can be given by

$$\overline{C_S^2}(y) = (C_{SR}^2(y) + C_{SI}^2(y))/2 \tag{22}$$

where C_{SR} and C_{SI} are the real and imaginary parts of $\overline{C_S}$ given by Eq. (20). It should be noted that the number of chord-wise and span-wise panels should be more than 30 in order to obtain a converged solution of $\overline{C_{TL}}$.

$\overline{C_{TD}}$ can be given by

$$\overline{C_{TD}} = \overline{T_D}/(\tfrac{1}{2}\rho U^2 S)$$
$$= \frac{1}{T^*}\int_0^{T^*}\left\{\iint_S \mathrm{Re}(\overline{\Delta P}(X,Y)e^{i\omega T})\,\mathrm{Re}(\frac{\partial F}{\partial X})dXdY\right\}dT/(\tfrac{1}{2}\rho U^2 S) \tag{23}$$

where Re indicates the real part of a complex quantity and T* is the period of the forced oscillation. We can easily derive the working form of $\overline{C_{TD}}$ by substituting Eq. (17) and the complex form of Eq. (1) into Eq. (23). The time mean necessary power coefficient $\overline{C_{PW}}$ can be given by

$$\overline{C_{PW}} = \overline{W}/(\tfrac{1}{2}\rho U^3 S)$$
$$= -\frac{1}{T^*}\int_0^{T^*}\left\{\iint_S \mathrm{Re}(\overline{\Delta p}(X,Y)e^{i\omega T})\,\mathrm{Re}(\frac{\partial F}{\partial T})dXdY\right\}dT/(\tfrac{1}{2}\rho U^3 S) \tag{24}$$

where $\overline{W}$ is the time mean rate of work. We can easily derive the working form of $\overline{C_{PW}}$ by substituting Eq. (17) and the complex form of Eq. (1) into Eq. (24). Then the propulsive efficiency η_p is defined by

$$\eta_p = \frac{\overline{TU}}{\overline{W}} = \frac{\overline{C_T}}{\overline{C_{PW}}} \tag{25}$$

III. Optimum Aeroelastic Design Using the Complex Method

By combining the general method for computing the aeroelastic effects of an elastic flapping wing, described in the previous section, and an optimization algorithm, we can conduct an optimum structural design of a flapping wing. For the optimization algorithm, we employed the complex method, originally proposed by Box [6]. The complex method is a direct search method that can handle multiple constraints without recourse to gradients. In the present study, we applied the optimization procedure to the design of a bird-like UAV that flies slowly like a Kite Hawk (Milvus migrans). As is well known, Kite Hawk is an expert of an efficient flight, namely, it finds the thermal convection and can perform continuous flight only by occasional flapping. If we could develop an UAV which imitates such flight of Kite Hawk, it might provide a highly efficient (long duration) UAV. In Fig. 3, the planform and structural arrangement of the semispan wing of the Kite Hawk

UAV are shown. The full span of the wing is 1.68 m and the root chord length is 0.28 m. The full span aspect ratio and wing area are 6 and 0.471 m^2, respectively. The total mass of the UAV is assumed to be about 300 g. The wing can sustain a total weight of 2.94 N at a cruising speed of 4.13 m/s at $C_L = 0.598$. The structural component consists of only a straight main-spar that can bend and twist and which is located near the leading edge, as shown in the Fig. 3. The ribs are assumed to be firmly attached to the main spar and are chord-wise rigid. It is assumed that the flapping wing motion is caused only by the dihedral flapping motion of the main spar. Therefore, the feathering motion is induced only by the aeroelastic response.

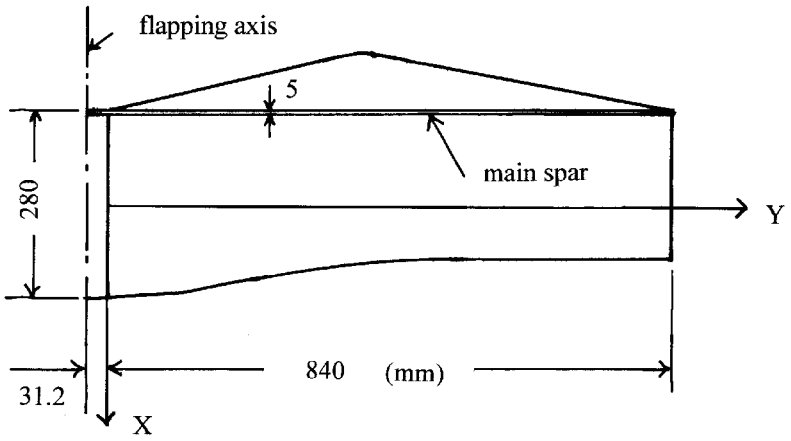

Fig. 3 Planform of Kite Hawk (Milvus migrans) UAV.

The purpose of the optimization study is to determine the thickness distribution of the main spar that generates the ideal bending and twisting motions to attain maximum propulsive efficiency. The section of the main spar is assumed to be rectangular and its width is assumed to be a constant 5 mm in the span-wise direction. The thickness distribution is assumed to be a parabolic function of y. We select thicknesses t_1, t_2 and t_3 at the root, mid-semispan and tip stations, respectively, as design variables to determine the structural characteristics. In addition to these design variables, we select k, ϕ_0 and a as design variables that determine the flapping wing motion. Therefore, there are six design variables in total. The objective function is the propulsive efficiency η_p. The following constraints are imposed, $\overline{C_T} \geq C_D$ and $t_1 \geq t_2 \geq t_3$, where C_D is the total drag coefficient of the UAV. Since the flapping wing is composed of a single-spar, we employ simple beam theory [7] to compute the natural vibration modes. The distributions of the mass m, static unbalance S_y and the moment of inertia I around the main spar are taken to be the concentrated quantities at the center of

the segment obtained by dividing the main spar into 13 equally spaced portions. It should be noted that the inetial data of the main spar itself changes at each iteration step of the optimization process. The value of the concentrated mass, imbalance and inertia at each segment are assumed to be equal and given as $m_i = 0.005$ kg, $Sy_i = 7.0\times10^{-5}$ kgm and $I_i = 5.0\text{x}10^{-5}$ kgm^2, for i = 1−13. The main spar is assumed to be a quasi-isotropic laminate construction of CFRP with elastic properties E_L = 181 Gpa, E_T = 10.3 GPa, G_{LT} = 7.17 GPa and $\nu = 0.28$.

In the present problem we set C_D to be 0.15. This value is considerably higher than the value of 0.055 estimated by the DLM code (assuming a minimum drag coefficient of 0.04 and an induced drag coefficient of 0.015 at $C_L = 0.598$). However, we assumed the DLM code would underestimate C_D as it does not account for viscous effects. This choice of C_D=0.15 will be justified in the next section by the numerical simulation using a Navier−Stokes code.

A converged solution was obtained after 50 iterations. The results were as follows:

$\eta_p = 0.754$, $\overline{C_T} = 0.166$ ($\overline{C_{TL}} = 0.089$, $\overline{C_{TD}} = 0.077$),

$\overline{C_{PW}} = 0.220$,

$k = 0.213$, $\phi_0 = 48.9$ deg., $a = -0.986$,

$t_1 = 5.76$ mm, $t_2 = 2.08$ mm, $t_3 = 0.92$ mm

The propulsive efficiency of 75% seems quite high. (Note that 75% of η_p is obtained for mean angle of attack 0 deg. Therefore, the induced drag due to the averaged lift is not taken into account in evaluating η_p.) Since the optimum value of the reduced frequency is 0.213, we can easily determine the cruising velocity to be U_C = 4.13 m/s by assuming a forced flapping frequency of 1 Hz. We can then easily estimate $C_L = 0.598$ to sustain a weight of 2.94 N at U_C = 4.13 m/s. The time mean necessary power $\overline{W}$ is 4.47 W and the power–mass ratio for this UAV is 14.9 W/kg, which seems quite efficient. The natural frequencies of the wing are f_1 = 1.65 Hz (1st bending predominant), f_2 = 5.93 Hz (1st torsion predominant), f_3 = 13.7 Hz (2nd torsion predominant). The six total natural vibration modes are employed in computing the aeroelastic responses. In Figs. 4, the wing deformations during one cycle of oscillation are shown. (Note that the wing displacement shown in Fig. 4 is not exaggerated.) As can be seen, the wing is very flexible and bends in the span-wise direction and twists around the main spar. From animations of the wing deformation sequence we can confirm that a span-wise traveling wave is generated.

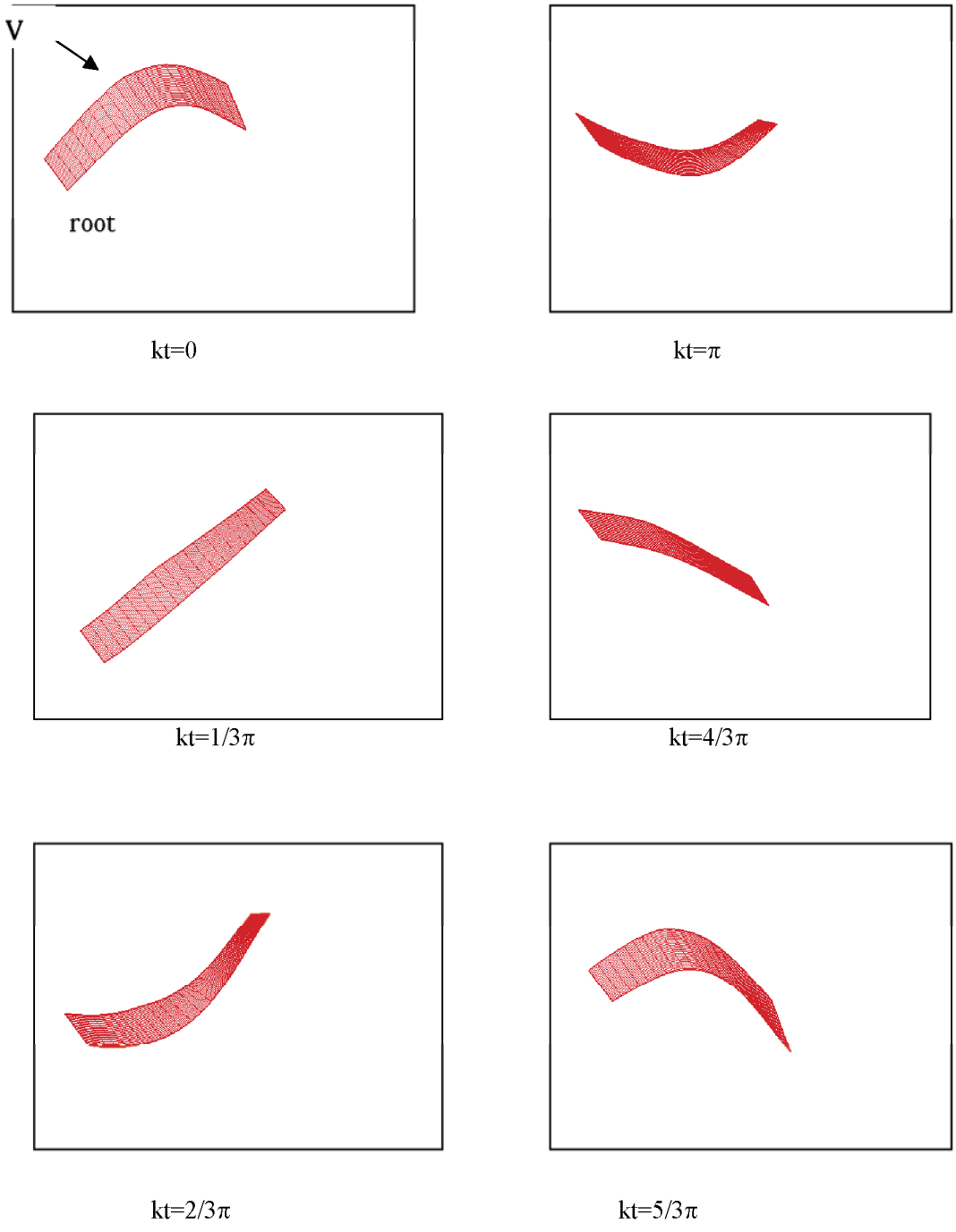

Fig. 4 Wing deformation during one cycle of oscillation.

IV. Numerical Simulation of Kite Hawk UAV Using Navier–Stokes Code

In order to evaluate the viscous effect on the optimum design of the Kite Hawk UAV, which is obtained using DLM as the aerodynamic tool, a numerical simulation was conducted using the three-dimensional Navier–Stokes (NS) code developed by Isogai [9]. Eq. (7) was incorporated into the NS code and the aeroelastic response of the wing was computed by solving Eq. (7) at each time step using the wing boundary condition (computed from the wing deformation obtained at one time step before). The natural vibration modes obtained for the optimum aeroelastic design described in the previous section were used for the aeroelastic response computation using the NS code. A C-H type structural grid system was used with 240 grid points in the chord–wise direction, 23 span-wise and 51 in the direction normal to the wing surfaces. The wing sections employed in the present NS simulation were generated by modifying the NACA0012 airfoil section by changing the thickness ratio, introducing camber and setting the maximum camber location. The amount of camber for local airfoil sections was changed parabolically from the root to the tip stations so that the camber at the root was maximum and that at the tip was zero. The thickness ratio of the present section was 6% and the maximum camber was 6% of the chord located 30% from the leading edge. The mean angle of attack was set as 8 deg, The Reynolds number based on the root chord was 7.63×10^4 and the Baldwin and Lomax algebraic turbulence model [10] was employed.

The results obtained are as follows:

$$\overline{C_T} = 0.046, \quad \overline{C_L} = 0.552, \quad \overline{C_{PW}} = 0.242$$

These coefficients give the following physical values at $U_C = 4.13$ m/s:

$$\overline{T} = 0.227\mathrm{N}, \quad \overline{L} = 2.71\mathrm{N}, \quad \overline{W} = 4.91\mathrm{W}$$

Based on these results, the wing can sustain a drag of 0.227 N and a weight of 2.71 N with a time mean power of 4.91 W and a power–mass ratio of 17.7 W/kg. These results show that the optimum aeroelastic design using DLM is still good even when viscous effects are taking into account. In Fig. 5, the wing deformations and flow patterns (iso-vorticity ω_y) during one cycle of oscillation are shown. In order to see the flow patterns in detail, the iso-vorticity distributions around the airfoil sections at 91% and 30% semispan stations are also shown in Figs. 6 and 7, respectively. As seen in Fig. 6, no flow separation is observed at 91% semispan station, which attains efficient thrust generation. However, as shown in Fig. 7, large scale flow separation can be seen at 30% semispan station, which seems to generate the drag. The flow separation observed in the inboard portion of the wing might be the main cause of the reduction of $\overline{C_T}$ compared with that predicted by DLM. In Figs. 8-10, the time histories of lift, thrust and rate of work during one cycle of oscillation are shown, respectively.

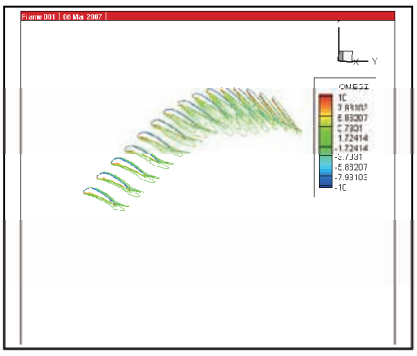

kt=0

kt=π

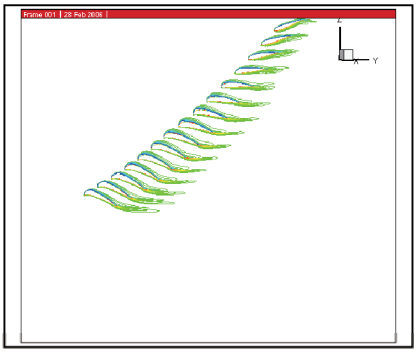

kt=1/3π

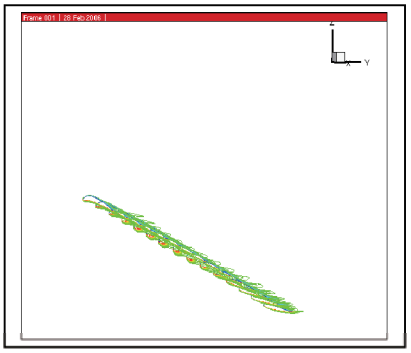

kt=4/3π

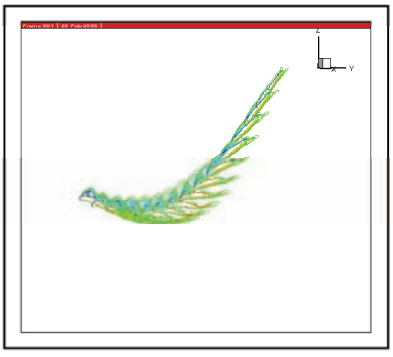

kt=2/3π

kt=5/3π

Fig. 5 Wing deformation and flow patterns (ω_y) during one cycle of oscillation.

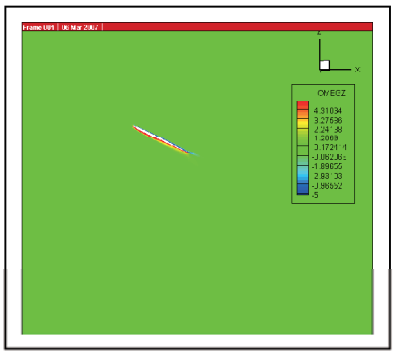

kt=0

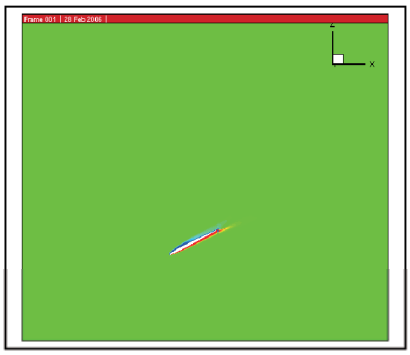

kt=π

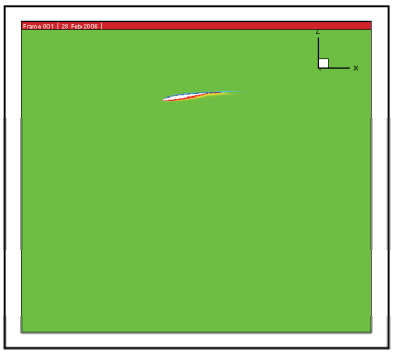

kt=1/3π

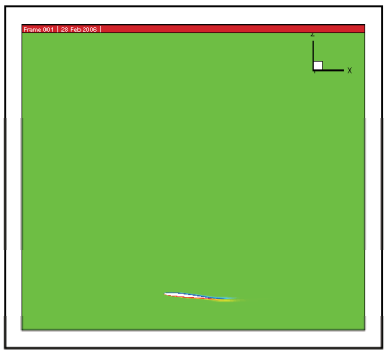

kt=4/3π

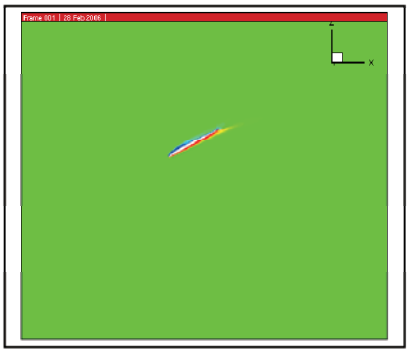

kt=2/3π

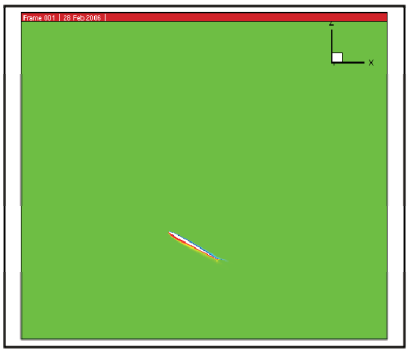

kt=5/3π

Fig. 6 Flow pattern (ω_y) at 91% semispan station.

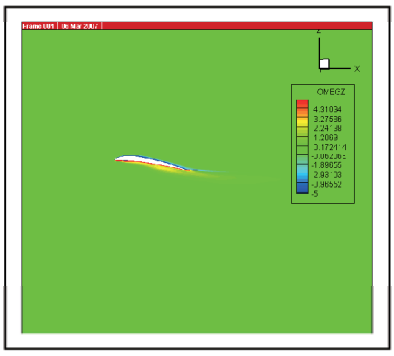

kt=0

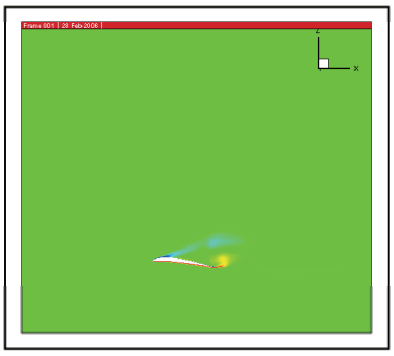

kt=π

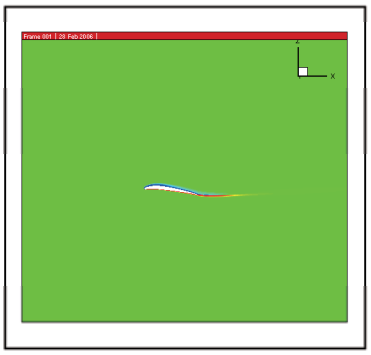

kt=1/3π

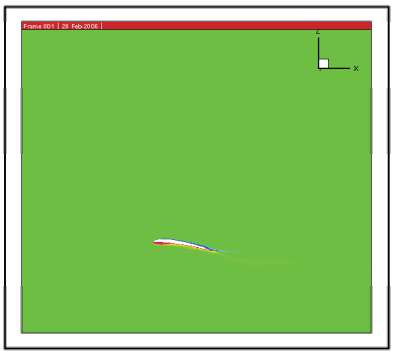

kt=4/3π

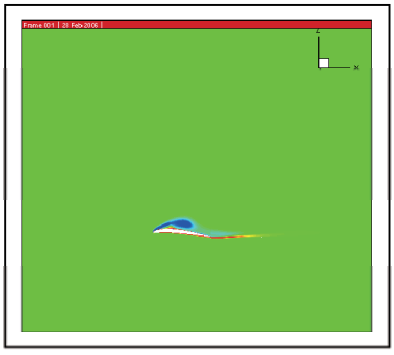

kt=2/3π

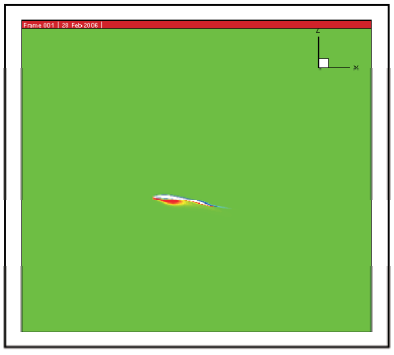

kt=5/3π

Fig. 7 Flow pattern (ω_y) at 30% semispan station.

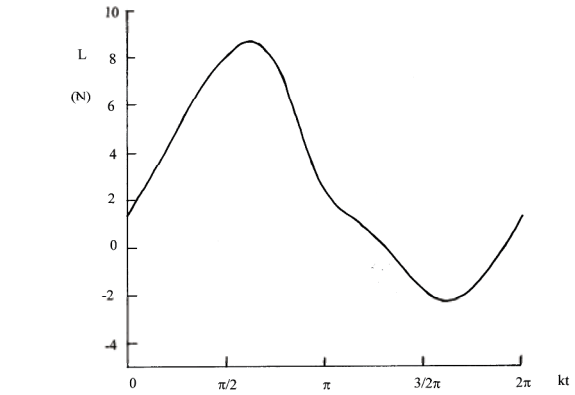

Fig. 8 Variation of lift during one cycle of oscillation.
$(\overline{L} = 2.71N)$

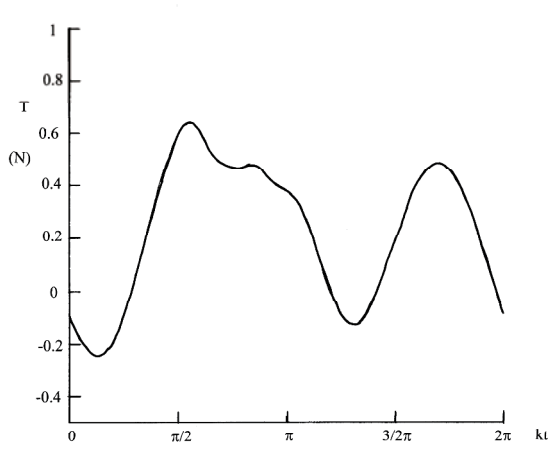

Fig. 9 Variation of thrust during one cycle of oscillation.
$(\overline{T} = 0.227N)$

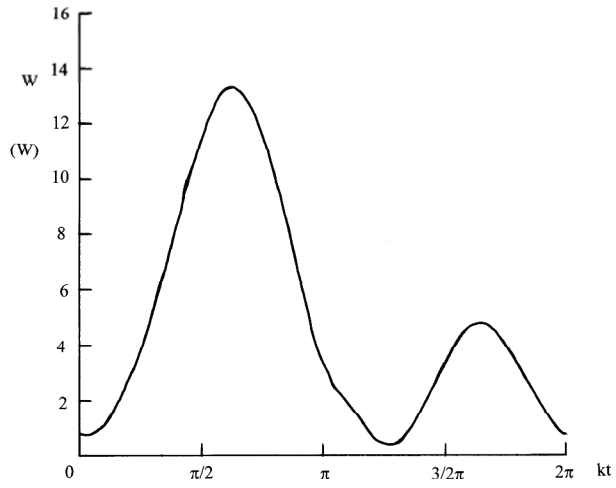

Fig. 10 Variation of rate of work during one cycle of oscillation. ($\overline{W} = 4.91W$)

V. Conclusion

A general method for the optimum aeroelastic design of a flapping wing employing lifting-surface theory as an aerodynamic tool and the complex method as the optimization algorithm is presented. The present optimum design method is applied to the Kite Hawk UAV and the optimum thickness distribution of the main-spar is determined. As a result of optimization, a high propulsive efficiency of 75% is attained considering only dihedral flapping of the main-spar. In order to evaluate the viscous effect on this optimum design using DLM, the numerical simulation using the Navier-Stokes code is conducted. It is found that the flow separation is suppressed around the out-board potion of the wing, that enables the efficient thrust generation, while the large scale flow separation is observed around the in-board potion, that degrades the propulsive efficiency. Although some degradation of the propulsive efficiency due to viscous effect is expected, it is believed that the present optimum design method using DLM might provide a useful aeroelastic design tool for a flapping wing of UAV.

References

[1] DeLaurier, J. D., and Harris, J. M., "A Study of Mechanical Flapping-Wing Flight," Aeronautical Journal, Oct. 1993, pp. 277-266.

[2] DeLaurier, J. D., "The Development of an Efficient Ornithopter Wing," Aeronautical Journal, May 1993, pp. 153-162.

[3] Albano, E., and Rodden, W. P., "Doublet-Lattice Method for Calculating Lift Distributions on Oscillating Surfaces in Subsonic Flows," AIAA Journal, Vol. 7, Feb. 1969, pp. 279-285.

[4] Lan, C. E., "The Unsteady Quasi-Vortex-Lattice Method with Applications to Animal Propulsion," Journal of Fluid Mechanics, Vol. 93, Part 4, 1979, pp. 747-765.

[5] Chopra, M. G., and Kambe, T., "Hydromechanics of Lunate-Tail Swimming Propulsion. Part 2," Journal of Fluid Mechanics, Vol. 79, part 1, 1977, pp. 49-69.

[6] Box, M. J., "A New Method of Constrained Optimization and a Comparison with Other Methods," Computer Journal, Vol. 8, 1965, pp. 42-52.

[7] Bisplinghoff, R. L., Ashley, H., and Halfman, R. L., Aeroelasticity, Addison Wesley, 1955.

[8] Beveridge, G.. S. G., and Schecheter, R. S., Optimization, Theory and Practice, Chemical Engineering Series, McGraw Hill, New York, 1970, pp. 453-456.

[9] Isogai, K., "Numerical Simulation of Unsteady Viscous Flow Around a Flapping Wing," Computational Fluid Dynamics 2002, Proceedings of the Second International Conference on Computational Fluid Dynamics, ICCFD, Sydney, Australia, July 2002, pp. 701-706.

[10] Baldwin, B. S., and Lomax, H., "Thin Layer Approximation and Algebraic Model for Separated Turbulent Flows," AIAA Paper 78-257, Jan. 1978.